Research Square

Preprints are preliminary reports that have not undergone peer review.
They should not be considered conclusive, used to inform clinical practice,
or referenced by the media as validated information.

Effects of heat-induced aggregation on the molecular structure of walnut glutelin and the digestibility of encapsulated β-carotene

Qian Sun
Qujing Normal University
Jing Wang
jingwang13579@163.com

Qujing Normal University

Research Article

Keywords: walnut glutelin (WG), heat aggregation, interfacial properties, protein emulsion, stability, β-carotene, in vitro digestion

Posted Date: November 13th, 2026

DOI: https://doi.org/10.21203/rs.3.rs-11263861/v1

License: This work is licensed under a Creative Commons Attribution 4.0 International License.
Read Full License

Additional Declarations: No competing interests reported.

Abstract

This study investigated the effects of thermal treatment on structural changes in walnut glutelin (WG), the interfacial properties of the resulting emulsion (oil-water interfacial adsorption), and the digestibility of embedded, encapsulated *β*-carotene. The results showed that heat treatment partially unfolded, denatured, and aggregated WG. Furthermore, heat-treated WG exhibited increased solubility, particle size, emulsifying properties, and surface hydrophobicity. The microstructure confirmed molecular aggregation. At the same time, fluorescence and infrared spectroscopy indicated that the secondary and tertiary structures of WG were disrupted, intramolecular hydrogen bonds were broken, and spectral red-shifts occurred, and those formed with heat-treated WG showed no signs of phase separation. Microstructural observations showed smaller, more uniform, droplets and higher interfacial protein adsorption, and that these emulsions were more stable. In *β*-carotene encapsulating emulsions, heat-treated walnut glutelin (WG) further enhanced *β*-carotene encapsulation and sustained its release.

Introduction

In protein production applications, heat treatment is an indispensable process for various protein types during food processing. For example, high-temperature sterilization, anti-nutritional factor inactivation, and spray drying can alter the natural protein structure, thereby significantly affecting protein functional properties and application value (Huang et al., 2025). Proteins are polypeptides with stable three-dimensional structures, and their conformational stability depends on various intermolecular forces (including hydrophobic interactions, van der Waals forces, hydrogen bonds, disulfide bonds, and others). During heat treatment, protein conformation changes (e.g., unfolding and aggregation) (Prates et al., 2018), with higher-order structure unfolding, exposure of hydrophobic residues, and increased surface sulfhydryl groups. This alters the ratio of hydrophilic to hydrophobic groups on the protein surface, causing the protein to lose its biological and functional properties. It typically disrupts forces that stabilize protein structure, including hydrogen bonds, hydrophobic interactions, electrostatic interactions, and disulfide bonds, altering protein structure and function (Guo et al., 2017). As temperature increases, the tightly ordered tertiary structure of proteins is disrupted first, causing the molecules to unfold and expose many hydrophobic amino acid residues, which facilitates intermolecular association through hydrophobic interactions. In addition, protein molecules undergo thiol or disulfide bond exchange reactions. (Mori et al., 2010). prepared thermal aggregates of 11S globin at 100°C and found that the acidic and basic subunits of 11S globin dissociated, resulting in increased solubility.

(Alizadeh-Pasdar & Chan, 2000). prepared thermal aggregates using BLG and bovine serum albumin at pH 3.0, 5.0, 7.0, and 9.0, respectively, and found that the surface hydrophobicity of BLG increased at all pH levels. (Muragama & Tomida, 2004). investigated the changes in the secondary structure of bovine serum albumin during thermal denaturation. They found that as the temperature increased, the proportion of *α*-helices in bovine serum albumin decreased, whereas the proportions of *β*-sheets and *β*-turns increased. (Zhou et al., 2017) demonstrated using Fourier-transform infrared spectroscopy (FTIR) that the hydrogen bonds in the thermal aggregates of 11S globulin at 95°C were stronger than those in

the untreated sample, as evidenced by an increase in β-sheet content. Therefore, understanding how the chemical bonds mentioned above change during thermal processing is crucial to elucidating the mechanisms by which thermal aggregation alters protein's physicochemical properties.

Proteins aggregate during heat treatment, denaturing and altering their structures and causing them to exhibit different sizes and surface hydrophobicity than in their native states. To better understand the relationship between the structure and functional properties of thermally denatured proteins, researchers are paying increasing attention to the digestion behavior of proteins after thermal aggregation. (Peram et al., 2013) studied the digestion behavior of BLG aggregates at different temperatures and found that BLG, after being heated at 90°C for 120 min, formed aggregates that were then almost completely digested by simulated gastric juice. (Liu et al., 2022) found that heat treatment caused partial unfolding of the BLG's spatial conformation; after 10 minutes, the degree of hydrolysis increased, and the activation energy for sensitivity to trypsin hydrolysis rose significantly. (Deng et al., 2020) found that heat treatment modifies β-lactoglobulin structure, resulting in higher gastric digestibility. (Tang et al., 2022) evaluated soybean and pea proteins heated at 65–100°C. They found that as the heating intensity increased, the surface hydrophobicity of the soybean and pea proteins increased. The digestibility of soybean protein increased from 30% (untreated) to 60%, whereas the digestibility of pea protein increased from 52% to 65%. Surface hydrophobicity was closely correlated with overall digestibility. (Lin et al., 2020) used pepsin and trypsin to hydrolyze both non-heated and heated hemp isolate proteins. They found that heat treatment increased low-molecular-weight protein levels and the degree of hydrolysis. Heat treatment significantly improved the digestibility of hemp protein isolates.

Walnut glutelin is the primary protein in walnuts, accounting for 70% (w/w) of their protein content (Sun et al., 2018). Walnut glutelin is rich in essential amino acids, and its nutritional value is comparable to that of soy protein (Sun et al., 2018). Walnut glutelin is a novel protein, and limited research on its functional properties has hindered its widespread use in the food industry. Heat treatment is common in the food industry, as most foods require heating to extend shelf life. Furthermore, although numerous studies have examined the effects of thermal aggregation on protein digestibility, no research has investigated the digestibility of thermally aggregated walnut glutelin. This study used heat treatment to prepare thermally aggregated walnut glutelin, analyzed the thermal aggregation behavior of walnut glutelin, investigated the patterns of change in physicochemical properties (such as solubility and emulsification properties), and elucidated the effects of heat treatment on protein structure and properties, with the aim of developing more functional food ingredients derived from walnut glutelin.

Materials and methods

Chemicals and reagents

Walnut (Yunnan Ludian cultivar) and walnut glutelin (laboratory-prepared, protein content 90%) were used in this study. Soybean oil was supplied by Yihai Kerry Arawana Holdings Co., Ltd.

Materials used were as follows

Bovine serum albumin, Beijing Solaibao Technology Co., Ltd. Potassium bromide (spectral grade), Tianjin Jinbeier Technology Co., Ltd. Nile Red and Nile Blue dyes, Sigma Aldrich (Shanghai) Trading Co., Ltd. *β*-carotene (BC) was purchased from Shanghai Yien Chemical Technology Co., Ltd. Methanol, n-hexane, dimethyl sulfoxide, dichloromethane, etc. (chromatographic grade) purchased from Sinopharm Chemical Reagents Co., Ltd. Non esterified fatty acid test kit, Suzhou Keming Biotechnology Co., Ltd. All other reagents were analytical grade.

Equipment used was as follows

FE 28 pH meter (Mettler Toledo Instruments (Shanghai) Co., Ltd). Kjeltec 8400/FOSS Fully Automatic Kjeldahl Nitrogen Analyzer (FOSS A/S, Denmark). F-7000 Fluorescence Spectrophotometer (Hitachi, Japan). TENSOR II Fourier Transform Infrared Spectrometer (Bruker, Germany). Nova Nano SEM 230 Scanning Electron Microscope (Shanghai Yuzhong Industrial Co., Ltd). Zeiss LSM880 Confocal Laser Scanning Microscope (Carl Zeiss, Germany). IKA T10 High-Speed Disperser (IKA, Germany). Malvern Zetasizer Nano ZS90 Zeta Potential Analyzer (Malvern, UK). Mastersizer 3000 Laser Particle Size Analyzer (Malvern, UK). LUMi Fuge (ILU1-LF111) Stable Analyzer (LUM, Germany).

Preparation of Walnut glutelin (WG)

WG was prepared according to the method described by Sun with slight modifications (Sun et al., 2018). After deglazing the walnut dregs, we added deionized water. After centrifugation, the supernatant was collected, and the remaining precipitate was treated with NaCl. The supernatant was re-extracted after centrifugation. The extract was treated with 70% ethanol and NaOH to adjust the pH. After centrifugation, the supernatant was adjusted to the isoelectric point with HCl. The extract was washed to neutral pH and vacuum freeze-dried to obtain WG (Sze-Tao & Sathe et al, 2000). The final protein content of the prepared WG exceeded 90%.

Heat treatment of WG

Walnut glutelin heat treatment: A walnut glutelin aqueous solution was prepared, diluted to 1 mg/mL, magnetically stirred at 25°C for 2–4 h, and then allowed to hydrate thoroughly at 4°C for 24 h. The protein solution was subjected to heat treatment at different temperatures (0, 60, 70, 80, 90, and 100°C) for 30 min (pH 7.0). After heat treatment, rapidly cool to room temperature in an ice-water bath, then centrifuge at 10,000 g for 30 min to remove precipitate and insoluble proteins, yielding heat-treated walnut glutelin (HT-WG). Store the aqueous solution at 4°C for later use.

Comparison of protein molecules before and after heat treatment

Solubility and particle size: We prepared an aqueous WG solution and diluted it to 1 mg/mL. The mixture was stirred magnetically at 25°C for 60 min (pH 7.0), centrifuged at 3,600 r/min for 20 min, and the supernatant was collected. The next 5 mL of supernatant was collected, and protein content was determined using the Kjeldahl method (conversion factor: 6.25 for soy protein). The particle size was determined using a Malvern Zetasizer 3000. The protein aqueous solution was filtered through a 0.45 μm water-based filter membrane, and the diluted solution was placed in a cuvette for analysis. With an extinction coefficient of 10%-15%, the particle size was measured at 25°C, and the results were expressed as $d_{4,3}$. Each sample was measured three times.

Emulsifying properties: Emulsifying Activity Index (*EAI*, m^2/g) and Emulsifying Stability Index (*ESI*, %): A 40 mL aliquot of a protein solution with a concentration of 10 mg/mL was mixed with 10 mL soybean oil (oil phase volume fraction ϕ) and emulsified at 10,000 r/min for 2 min. Fifty microliters of the emulsion were collected from the bottom of the test tube, diluted and mixed, and the absorbance A_0 (absorbance at 0 min) was measured at a wavelength of 500 nm. The control group consisted of a 0.1% SDS solution (Pearce & Kinsella, 1978). After allowing the emulsion to stand for 10 min, the emulsion was aspirated from the bottom of the test tube, and the absorbance A_{10} was measured using the method described above. *EAI* (m^2/g) = $[2 \times 2.303 / c \times \phi \times 10^4] \times A_0 \times 100$, *ESI* (%) = $A_{10} / A_0 \times 100$

Mercaptan (-SH) content

The protein solution was taken, and 0.05 mL of β-mercaptoethanol and 4 mL of 8 M urea solution were added, and it was incubated in a water bath at 25°C for 1 h. Then, 10 mL of 12% TCA was added; the mixture was incubated in a water bath at 25°C for another hour. Centrifuge the mixture was at 10,000 r/min for 10 min. The sample was centrifuged to remove β-mercaptoethanol, and this step was repeated twice. The precipitate was dissolved in 0.1 mol/L phosphate buffer; 0.08 mL of DNTB was added; the mixture was shaken vigorously and vortexed; incubated in a water bath at 25°C for 1 h; and centrifuged at 10,000 r/min for 30 min. The control group contained no DNTB. The absorbance was measured at a wavelength of 412 nm (supernatant), and the thiol content was calculated using an extinction coefficient of 13,600 M^{-1} cm^{-1} (the molar extinction coefficient of Ellman's reagent, 106/1.3600 = 73.53). *-SH* (μmol/g) = $73.53 \times A_{412} \times D_1 / C$. *D* is the dilution factor; D_1 is 2.03, and *C* (mg/mL) is the final protein concentration of the sample.

Surface hydrophobicity

The protein was diluted to different concentrations. Next, add 20 μL of 8.0 mM ANS to 4 mL of protein samples at various concentrations. The excitation wavelength was set to 390 nm, the scanning range was 400–600 nm, and the slit width was 5 nm. We plotted fluorescence intensity against protein concentration, and the slope of the line represented the protein sample's surface hydrophobicity.

Microstructural observation

A volume of 20 μL of the diluted protein sample was placed on a silicon wafer. After the water evaporated, the wafer was placed on a sample stage coated with a conductive adhesive, then gold-sputtered for 90 s and imaged at 20 kV using a Scanning Electron Microscope (SEM).

Fluorescence spectroscopy: The protein solution was diluted to a concentration of 0.1 mg/mL, with an excitation wavelength of 290 nm, an emission wavelength measurement range of 240–480 nm, a scan rate of 1,200 nm/min, and excitation and emission slit widths of 5 nm (Zheng et al., 2020). Fourier transform infrared spectroscopy: resolution of 4 cm^{-1}, wavenumber accuracy of 0.01 cm^{-1}, ambient temperature of 25°C, 32 scans across the full wavelength range (4,000-400 cm^{-1}), with software calibration to remove interferences such as water vapor and carbon dioxide.

Emulsion formation and stabilization before and after heat treatment

WG emulsion preparation

Prepare a 3.0 wt.% aqueous protein solution (pH 7.0), stir magnetically for 2–4 h, and hydrate at 4°C for 24 h until the WG is completely dissolved. Dilute to a 1.0 wt.% aqueous protein solution, adjust the pH to 7.0, and add soybean oil to achieve an oil phase ratio of 0.20 (v/v, oil phase volume fraction ϕ = 20). Process the mixture at 16,000 r/min for 20 s to form a walnut glutelin emulsion (WG emulsion).

WG emulsion properties: Appearance and Creaming Index (*CI* / %): Take 6 mL of the prepared emulsion and place it in a transparent round-bottom bottle and leave it at 25°C for 0 d (24 h). The emulsion separation was calculated using photographs. By measuring the ratio of the height of the lower clear phase, H_s, to the total height, *H*, *CI* (%) = H_s / *H*. We used the Malvern Mastersizer 3000 to analyze the droplet size $d_{4,3}$, opacity 10%-15%, emulsion refractive index 1.095, and aqueous-phase refractive index 1.330. The microstructure of the emulsion was observed using an LSM880 optical microscope. The aqueous phase (protein) and oil phase (soybean oil) were stained with Nile Blue and Nile Red, respectively, at excitation wavelengths of 488 and 633 nm. We processed the images using ZEN 2 software. After processing, the protein appeared pink, while the oil appeared blue or light blue (Chen et al., 2019).

Interfacial protein adsorption

The initial total protein concentration C_0 (mg/mL) in the emulsion was determined. The emulsion (2 mL) was transferred to a centrifuge tube and centrifuged at 10,000 g for 30 min. The supernatant was collected from the bottom of the tube, filtered through a 0.22 μm syringe filter, and the protein concentration, C_s (mg/mL), was determined using the Kjeldahl method (Liang & Tang, 2014). Emulsified protein content C_0-C_s (mg/mL); interfacial protein adsorption rate *AP* (%) = (C_0-C_s) / C_0 × 100; interfacial protein adsorption amount Γ = (C_0-C_s) / *A* (*A*, specific surface area of droplets, m^2/mg)

WG emulsion stability

Emulsion stability was evaluated using a LUMiSizer stability analyzer (Li et al., 2018). A 420 μL sample of the fresh emulsion was transferred to a PC sample cell with a 2 mm optical path length. Centrifugation was used to accelerate the internal flow rate of the emulsion, and the transmittance of the emulsion was measured. The centrifugation speed was 1,000 r/min, the centrifugation time was 50 min, the temperature was 25°C, and the emulsion was scanned every 10 s.

β-carotene in composite emulsions

Composite emulsion preparation

A 1.0 wt.% aqueous protein solution (pH 7.0). *β*-carotene was dissolved in soybean oil and stirred magnetically for 24 h until fully dissolved, yielding a 0.1% (w/w) solution. The oil phase ratio was 0.20 (oil phase volume fraction ϕ = 20) with added soybean oil (containing 0.1% *β*-carotene). The mixture was treated at 16,000 r/min for 20 s to form a composite emulsion (WG-BC), which was stored at 4°C until needed. During preparation and storage, all containers were dark brown serum bottles wrapped in aluminum foil to minimize *β*-carotene loss.

β-carotene detection: Prepare *β*-carotene standard solutions with concentrations of 0.1–100 μg/mL. The regression equation for the calibration curve was derived from peak areas and standard concentrations, yielding R^2 > 0.99. We calculated the *β*-carotene content in the sample using the standard curve. HPLC determination of *β*-carotene and other compounds was performed. The ultracentrifugation method was followed as described by (Moharana et al., 2025). HPLC separation conditions: temperature 25°C, column temperature 10°C, flow rate 1 mL/min, injection volume 20 μL, and detection wavelength 450 nm. Chromatographic conditions: Mobile phase A, methanol/acetonitrile/ultrapure water (84/14/2, v/v/v); eluent B, dichloromethane. The flow rate was 1.0 mL/min. The A to B ratio was 80:20 at 0 min, 45:55 from 0 to 20 min, and 80:20 from 20 to 28 min.

In vitro gastrointestinal digestion model

We constructed a gastrointestinal digestion model based on the system described by (Lakemond et al., 2000). Before the experiment, all solutions were preheated to 37°C and maintained at 37°C throughout. Emulsion to be digested: oral juice: simulated gastric juice: simulated intestinal fluid volume ratio is 1:1:1:2. The pH range of 6.8-7.0 was simulated during the oral digestion phase, incubated continuously at 120 r/min, and samples were taken at regular intervals. The gastric digestion phase was simulated at 180 r/min, incubated continuously, and sampled at regular intervals. During the simulated intestinal digestion phase, at pH 7.0 (to terminate the gastric digestion reaction), incubation was performed at 150 r/min, with samples collected at regular intervals.

β-carotene release rate: Digestive samples simulating gastric and intestinal fluids were collected at predetermined time intervals, and the pH was adjusted to inhibit sample digestion. *β*-carotene content was determined using the method described by (Moharana et al., 2025). The digested samples were

mixed with n-hexane and vortexed for 10 s to extract free *β*-carotene from the aqueous phase; the extraction was performed 3 times. Release rate (%) = amount released during digestion/amount in the digestion fluid × 100.

Bioavailability (Bioaccessibility): The *β*-carotene content m_0 / g in the original emulsion; the *β*-carotene content m_1 / g in the digestate after digestion, centrifuged at 4°C and 10,000 g for 40 min. The top layer consisted of a thin layer of oil or a cream; the middle layer was a micellar phase (*β*-carotene content of m_2 in the micellar phase); and the bottom layer consisted of insoluble matter. 5 mL of the micellar phase and pass it through a 0.45 μm microporous filter membrane. The filtrate (emulsion) was mixed with dimethyl sulfoxide at a 1:1 volume ratio, and a vortex mixer was used to break the emulsion. Dichloromethane/n-hexane (1:4, v/v) was added, vortexed for 30 s, and centrifuged at 3,000 g for 5 min. The supernatant was transferred, and the concentration of extracted *β*-carotene was determined at 450 nm. Bioavailability (%) = *β*-carotene content in the micellar phase / *β*-carotene content in the digestive fluid × 100.

Statistical analysis

Graphs were generated using Origin 8.5 (2010), and statistical analyses were performed using SPSS version 19.0 (IBM Corp., Armonk, NY, USA). We analyzed differences among groups using one-way analysis of variance (ANOVA), followed by Duncan's multiple range test for post hoc comparisons. A $p < 0.05$ was considered statistically significant. The Confocal Laser Scanning Microscopy (CLSM) results were processed using ZEN 2 (Blue Edition) software, in which proteins appeared pink and lipids appeared blue or light blue. Unless otherwise specified, all experiments were performed with at least three independent replicates.

Results and discussion

Effect of heat-processed on the molecular properties of WG

Table 1 Effect of heat-processed on the molecular properties of WG

Table 1
Effect of heat-processed on the molecular properties of WG

Index	*Solubility*/%	*EAI*/%	*ESI*/%	$d_{4,3}$/nm	-*SH*μmol/g	H_0μmol/g
WG	16.14 ± 0.67^{jk}	76.51 ± 4.64^{d}	90.17 ± 6.02^{b}	75.43 ± 4.31^{j}	$2.05 \pm 0.11_{a}$	784.32 ± 49.72^{gh}
HT-60	21.42 ± 2.02^{ij}	79.16 ± 5.58^{cd}	96.97 ± 5.95^{a}	126.29 ± 9.89^{h}	1.96 ± 0.05^{ab}	953.51 ± 63.62^{ef}
HT-70	30.53 ± 2.43^{h}	87.23 ± 5.18^{b}	97.03 ± 6.33^{a}	$136.22 \pm 8.74_{h}$	1.84 ± 0.06^{b}	1287.65 ± 75.63^{b}
HT-80	49.87 ± 3.51^{d}	90.55 ± 5.34^{ab}	98.14 ± 6.46^{a}	146.95 ± 10.33^{gh}	1.65 ± 0.02^{bc}	1395.48 ± 80.05^{a}
HT-90	63.56 ± 4.46^{ab}	92.68 ± 6.09^{a}	98.05 ± 7.03^{a}	233.55 ± 14.59^{de}	1.71 ± 0.09^{bc}	1353.42 ± 79.57^{cd}
HT-100	66.45 ± 4.24^{a}	94.26 ± 6.12^{a}	98.42 ± 6.92^{a}	222.08 ± 10.95^{a}	1.79 ± 0.08^{b}	1364.83 ± 68.85^{ef}

Note: WG stands for walnut gluten, c = 1.0%; ϕ = 20. Heat treatment (HT): 60, 70, 80, 90, and 100°C for 30 min. Solubility (%), emulsifying ability (EAI, %), emulsifying stability (ESI, %), volume-average diameter ($d_{4,3}$, nm), free thiol content (-*SH*, μmol/g), and surface hydrophobicity (H_0, μmol/g). Superscripts with the same column but different letters (a-k) indicate statistically significant differences among samples ($p < 0.05$).

Non-covalent bonds primarily hold insoluble proteins together, and heat treatment causes violent molecular vibrations. Heat weakens various intramolecular and intermolecular forces within protein molecules (hydrogen bonds, electrostatic interactions, van der Waals forces, and hydrophobic interactions). Intermolecular bonds were disrupted, and some insoluble proteins became soluble, with solubility increasing from 16.14 to 66.45 compared to the unheated state. When a protein solution is heated, its structure changes owing to hydrogen bonds and hydrophobic interactions within the protein. Changes in intramolecular interactions, such as disulfide bonds, lead to the unfolding of the higher-order structure, resulting in a more flexible structure; at this point, the protein's emulsifying properties are also correspondingly enhanced. During this process, hidden internal hydrophobic groups and sulfhydryl groups are gradually exposed, and the protein molecules interact through thiol exchange via disulfide bonds, forming the HT-WG aggregate. WG particles, with a particle size of 75.43 nm, polymerized into approximately spherical aggregates. Compared with natural WG, all heat treatments increased the average protein diameter, reaching a maximum of 233.55 nm (at 90°C). Some studies suggest that proteins adsorb to the oil-water interface and that free thiol groups between protein molecules may interact (Lakemond et al., 2000). In this study, the free thiol content of HT-WG was lower than that of WG. This may be due to the oxidation of free thiols or the formation of disulfide bonds (-*S*-*S*-) between free thiols during aggregate formation through heat treatment. Compared to WG, the aggregates exhibited greater surface hydrophobicity.

The hydrophobicity of a protein surface indirectly reflects its structure and properties, and effectively reflects its surface activity. The hydrophobicity index H_0 reflects the intensity of the excitation light following ANS binding to hydrophobic sites on the protein surface at a given protein concentration. Therefore, the larger the H_0, the greater the protein hydrophobicity (Tang et al., 2021). Heat treatment disrupts intramolecular hydrogen bonds in protein molecules, exposing hydrophobic side chains to the surface and increasing surface hydrophobicity (Tang et al., 2021). According to (Wang et al., 2021). when proteins are heated above 80°C, their internal hydrophobic groups become exposed, aggregation occurs, and surface hydrophobicity increases. As the same time, heat treatment increases WG solubility and enhances the surface hydrophobicity of soluble aggregates. These results indicate that the extent of WG structural unfolding and aggregation varies with treatment temperature.

Particle size distribution and microstructure

Figure 1 Effect of heat treatment on the particle size distribution of WG. WG is walnut glutelin; HT-90 is heat-treated walnut glutelin (90°C, 30 min).

Figure 1 in conjunction with Table 1. Compared with natural WG, heat treatment increased the average WG particle size. Heating caused some protein molecules to unfold and aggregate; consequently, the aggregate size of HT-WG increased and the peak broadened, reflecting the degree of protein aggregation under heat treatment (Liu & Tang, 2014; Wang et al., 2012). In addition, SEM microstructural analysis showed that the loose, irregular surface structure transformed into a dense, angular structure (1,000 X and 5,000 X magnification). At 20,000 X magnification, the heat-treatment (HT-WG) clearly shows significantly more aggregates than WG. This supports the finding that WG forms numerous aggregates upon heating, increasing the particle size $d_{4,3}$ (Table 1).

The Effect of heat treatment on the molecular structure of WG

Fluorescence spectra

Figure 2 Fluorescence spectroscopy Analysis. WG is walnut glutelin; black, red, orange, green, blue, and purple represent WG, HT-60, 70, 80, 90, and 100°C, respectively, for 30 min.

Fluorescence spectroscopy is commonly used to study changes in protein conformation. Fluorescence scanning spectroscopy in the 240–480 nm wavelength range can be used to characterize changes in the microenvironment surrounding tryptophan (Trp), tyrosine (Tyr), and phenylalanine (Phe) residues. The fluorescence spectrum generated at an excitation wavelength of 310 nm is primarily due to tryptophan in the proteins (Nyemb et al., 2014). After heat treatment, the fluorescence intensity of WG increased, and the fluorescence peak shifted toward the blue. Heat treatment exposes hydrophobic groups on the molecular surface of natural WG molecules, shifting them from polar to nonpolar and increasing surface hydrophobicity. The maximum fluorescence intensity was observed at 348 nm, and it decreased as temperature increased. Changes in fluorescence intensity may be attributed to differences in energy-

transfer efficiency between tryptophan and tyrosine, as well as to heat-treatment exposure of protein chromophores. Tryptophan, tyrosine, and phenylalanine residues in proteins exhibit fluorescence polarization that is highly dependent on protein folding. Therefore, the natural WG tertiary structure undergoes partial unfolding upon sustained heating above 70°C.

Infrared spectroscopy

Figure 3 Infrared spectroscopy analysis. WG is walnut glutelin; black, red, orange, green, blue, and purple represent WG, HT-60, 70, 80, 90, and 100°C, respectively, for 30 min.

The stability of protein structures depends on various types of chemical bonds, including hydrogen and disulfide bonds. This suggests that during heat treatment, the higher-order structure of WG is partially disrupted, and the sulfhydryl groups on the side chains are oxidized to form disulfide bonds. Figure 3 shows the infrared spectra of natural WG and heat-treated HT-WG. Heat treatment reduces the number of hydroxyl groups in the peptide chain. In the 3700 – 3000 cm^{-1} range, the peak widths were narrower than those of WG. This indicates that there may be a large number of intramolecular or intermolecular hydrogen bonds in WG. In addition, the spectral peaks also shifted. This indicates that heat treatment can directly affect the spatial structure of WG.

In the protein infrared spectra, the amide I and II bands are typically considered characteristic absorption bands, with wavelengths ranging from 1700 – 1600 cm^{-1} (Verma et al., 2021). The amide band I is primarily caused by the C = O stretching vibration. The band in amide spectrum II reflects intermolecular or intramolecular hydrogen bonding interactions. When hydrogen bonds are disrupted, the spectral band shifts toward higher wave-numbers, and the proportion of random coiled-up structure increases (Table 2); part of the protein's secondary *β*-sheet structure is converted into random coiled-up structure. In the amide II region near 1548 cm^{-1}, all HT-WG samples exhibited significant changes after heat treatment. This indicates that hydrogen bonds were broken and the secondary structure was no longer dominated by *β*-sheets. Simultaneously, the peak shifted. After heat treatment, the amide I band shifted to lower wave-numbers, indicating that HT-WG was thermally unstable. When hydrogen bonding is strong, the electron density of the C = O bond decreases, and the absorption peak shifts toward lower wavenumbers.

Table 2
Effect of heat treatment on the secondary structure of WG

heat treatment/°C	α-helix (%)	β-sheet (%)	β-turn (%)	Unordered (%)
WG	27.71 ± 1.95^{a}	26.44 ± 1.88^{bc}	30.77 ± 2.15^{a}	14.56 ± 1.11^{ef}
HT-60	26.95 ± 1.44^{a}	26.78 ± 2.05^{bc}	$29.94 \pm 2.53_{a}$	16.28 ± 1.89^{e}
HT-70	25.13 ± 1.56^{ab}	$27.16 \pm 1.88_{bc}$	27.65 ± 2.37^{ab}	19.55 ± 2.01^{d}
HT-80	19.37 ± 1.66^{cd}	29.41 ± 2.12^{ab}	29.45 ± 2.02^{a}	21.34 ± 1.77^{cd}
HT-90	$17.54 \pm 1.59_{d}$	30.33 ± 3.05^{ab}	22.86 ± 1.45^{c}	28.62 ± 2.44^{ab}
HT-100	16.82 ± 1.41^{d}	32.69 ± 2.56^{a}	19.71 ± 1.38^{d}	30.43 ± 2.78^{a}

Note: WG denotes walnut protein isolate; c = 1.0%; ϕ = 20. Heat treatment (HT): 60, 70, 80, 90, 100°C for 30 min. Superscripts with different letters (a-f) within the same column indicate statistically significant differences among samples ($p < 0.05$).

Table 2 Effect of heat treatment on the secondary structure of WG

In combination with Table 2, compared with natural WG, the α-helix content of heat-treated HT-WG significantly decreased from 27.71 to 16.82 ($p < 0.05$). As the heat treatment temperature increased, the structural stability of WG decreased. However, β-fold content increased slightly. According to the literature, heating increases the proportion of β-sheets, exposing more hydrophobic segments on the molecular surface and promoting protein self-assembly (Zhao et al., 2023). The random coil content increased from 14.56 to 30.43, indicating that heat treatment caused part of the protein's secondary structure to transition from an ordered structure to a random coil structure. Compared with WG, HT-WG showed an increase in β-fold and a decrease in β-turn content after heat treatment. These trends relate to WG denaturation and aggregate.

Preliminary research: Previous studies by the team indicated that natural WG contains a high proportion of glutelin. At 60°C, glutelin undergoes thermal denaturation, promoting intermolecular aggregation. As the temperature increases, alcohol-soluble proteins and glutelin in WG begin to denature. Larger aggregates (thermopolymers) gradually formed; the particle size increased rapidly ($d_{4,3}$ in Table 1), and the surface hydrophobicity increased. In addition, WG aggregates formed after heat treatment, decreasing α-helix content. This is primarily because heat treatment at higher temperatures exposes the hydrophobic groups within WG molecules, causing some β-turn structures to transition to random-coil conformations (Ren et al., 2022).

Characterization of WG emulsion

Appearance and microstructure

Figure 4 Direct photographs of WG emulsion (stored at 25°C for 24 h), particle size distribution, and microstructure (20 X). Protein particle signal was set to pink (488 nm), and the oil-phase droplets are visualized in blue (leaning toward blue-green, 633 nm). WG is walnut glutelin; c = 1.0%; ϕ = 20. Heat treatment: 60, 70, 80, 90, 100°C for 30 min.

As shown in Fig. 4, the emulsion was left for 24 h to observe its appearance. The WG emulsion exhibited creaming (phase separation) with 37.34% fat content. However, the HT-WG emulsion was stable, with a fat separation value of 6.98% at 60°C, whereas no fat separation occurred in the other emulsions. CLSM images showed spherical droplets, and the blue (blue-green) oil-phase droplets were enveloped by pink protein, forming a stable oil-in-water system. Slight droplet flocculation occurred in the HT-WG emulsions, with flocculation visible among smaller oil-phase droplets. The presence of large voids between the droplets indicates that “bridging” flocculation occurred between them. In addition, the droplet sizes exhibited an almost monomodal distribution, concentrated between 20 and 40 μm, indicating that the resulting emulsion was stable. Research has shown that large molecules exhibit higher convective mass transfer rates (Ren et al., 2022). High-speed homogenization tends to generate intense turbulence, promoting the rapid adsorption of protein aggregates at the oil-water interface. However, owing to steric hindrance within the aggregates, oil-phase droplets coalesce to form larger droplets (Guilmineau & Kulozik, Part 1 and Part 2, 2006).

Table 3 Volume average diameter ($d_{4,3}$/μm) of WG emulsions and interfacial properties before and after heat treatment

Table 3
Volume average diameter ($d_{4,3}$/μm) of WG emulsions and interfacial properties before and after heat treatment

heat treatment/°C	$d_{4,3}$/μm	*CI*/%	C_0-C_S/%	*AP*/%	Γ/m²/mg
WG	42.22 ± 2.95^{a}	37.34 ± 1.03	0.24 ± 0.02^{ab}	24.12 ± 5.17^{c}	0.1563 ± 0.01^{cd}
HT-60	32.56 ± 2.13^{c}	6.98 ± 0.21	0.27 ± 0.05^{ab}	26.91 ± 2.46^{bc}	0.2012 ± 0.02^{c}
HT-70	30.91 ± 2.42^{c}	0	0.30 ± 0.01^{ab}	30.22 ± 3.05^{b}	0.2847 ± 0.01^{b}
HT-80	25.46 ± 1.95^{d}	0	0.35 ± 0.03^{a}	35.47 ± 2.98^{a}	0.3032 ± 0.03^{a}
HT-90	16.75 ± 1.67^{ef}	0	0.38 ± 0.06^{a}	37.65 ± 3.32^{a}	0.3275 ± 0.02^{a}
HT-100	23.18 ± 1.34^{de}	0	0.38 ± 0.03^{a}	38.24 ± 4.95^{a}	0.3341 ± 0.04^{a}

Note: WG denotes walnut gluten, c = 1.0%; ϕ = 20. Heat treatment (HT): 60, 70, 80, 90, 100°C for 30 min. $d_{4,3}$ denotes the volume-average diameter of the emulsion. *CI*/% denotes the milk fat content. C_0-C_S/% denotes the emulsifying protein content. *AP*/% denotes the interfacial protein adsorption rate. Γ/m²/mg denotes the interfacial protein adsorption amount. Superscripts with the same column but different letters (a-f) indicate statistically significant differences among samples (p < 0.05).

The droplet size ($d_{4,3}$) in Table 3 shows that the $d_{4,3}$ of the WG emulsion was 42.22 μm. After heat treatment, the $d_{4,3}$ of the HT-WG emulsion was in the range of 16.75 μm-32.56 μm. Combining the changes in particle size and hydrophobicity in Table 1, the surface hydrophobicity of natural WG increased after heat treatment. Exposure of hydrophobic residues within protein molecules enhances emulsifying capacity (Gantumur et al., 2023). Consequently, its ability to form oil-in-water droplets improved. Compared to the WG emulsion, the HT-WG emulsion formed smaller and more uniform droplets after heat treatment. The HT-WG stabilized emulsion had a significantly higher content of interfacial proteins than the WG emulsion (Table 3).

(Keerati-u-rai & Corredig, 2009). compared the effects of heat treatment on protein content at the interface before and after soy protein emulsification and obtained similar results. Heat-treatment temperature significantly affects the amount and rate of protein adsorption at the interface. When the temperature was below 70°C, the interfacial protein content increased rapidly. However, above 70°C, interfacial protein content increased more slowly. Heat treatment may improve emulsion stability by altering the internal structure of WG molecules, making them more likely to bind tightly to the oil phase. A more robust structure was formed on the surface of the oil droplets, which inhibited emulsion stratification to some extent.

Stability Analysis

Figure 5 Emulsion stability analysis. WG is walnut glutelin; c = 1.0%; ϕ = 20. Heat treatment: 60, 70, 80, 90, 100°C for 30 min.

LUMiSizer is commonly used to compare and analyze emulsion stability by accelerating centrifugation. Above 70°C, the emulsion gradually became more stable (Fig. 5, with lower transmittance and a slower rise in the backscatter peak). However, emulsions formed from natural WG are relatively less stable and exhibit higher light transmittance. At temperatures above 80°C, there was no significant change in transmittance, and heat treatment had a minimal effect on the emulsion stability of WG. Both CLSM microstructural and LUM analyses indicated that emulsion stability related to WG molecular properties before and after heating, consistent with changes in appearance, morphology, and droplet size (Fig. 4 and Table 3).

In vitro Digestion

Physicochemical properties of the emulsion digestion process

Figure 6 Microscopic diagram of WG composite emulsion digestion (20 X). WG is walnut glutelin; HT-90 is heat-treated walnut glutelin (90°C, 30 min); c = 1.0%; ϕ = 20.

The release characteristics of the functional ingredients in composite emulsions are related to changes in particle size (Xie et al., 2019). In simulations of gastrointestinal digestion, the HT-WG composite emulsions showed similar droplet sizes ($d_{4,3}$), with a trend toward larger droplets. During simulated gastric digestion, droplets coalesce and aggregate extensively due to electrostatic interactions under acidic conditions (Fig. 6) (Zou et al., 2016). In emulsions, pepsin can hydrolyze WG, reducing electrostatic repulsion and steric hindrance and increasing droplet size. However, after 60 min of simulated gastric digestion, the droplet size of the HT-WG composite emulsion did not increase considerably (Fig. 6). This indicates that the composite emulsion formed by WG under acidic conditions is more stable than that formed by WG alone.

After digestion in intestinal fluid, the droplet size ($d_{4,3}$) of the composite emulsion decreased significantly, indicating that smaller droplets exhibit a higher rate of lipid hydrolysis than larger droplets. Therefore, when simulating intestinal fluid digestion, the number of smaller fat droplets decreases rapidly within the first 120 min. The droplet size distribution indicates that, after 120 min of intestinal digestion, the number of smaller fat droplets in the composite emulsion decreased (Fig. 6). The findings of the aforementioned studies also support the conclusion that the smaller the droplet size in an emulsion, the greater the rate and degree of lipid hydrolysis, which results in a smaller interfacial area of oil droplets exposed to lipase in the emulsion (Li & McClements, 2010; Singh & Ye, 2013). Compared to

digestion by gastric juice, the droplet size ($d_{4,3}$) of the WG composite emulsion decreased, indicating that most of the WG composite emulsion was digested during the gastric juice phase.

Changes during the emulsion digestion process

Figure 7 In vitro release and bioavailability of WG composite emulsion. WG stands for walnut glutelin; c = 1.0%; ϕ = 20. Heat treatment: 60, 70, 80, 90, 100°C for 30 min.

During digestion by gastric juices, the composite emulsion was broken down by pepsin, and BC in the composite emulsion was released during gastric digestion. The BC release rate of the HT-WG composite emulsion in gastric juice was only 35.52%-27.16%, and its release rate was slower than that of the natural WG composite emulsion. (Guo et al., 2020) found that an emulsion of pea protein and PT complex can delay the digestion of BC in the stomach. However, after 120 min of digestion in intestinal fluid, BC was released in large quantities from the HT-WG composite emulsion, with the release rate being highest at 73.47%. This results in a smaller interfacial area for lipase contact with emulsion droplets, facilitating lipase penetration of the lipid droplet surface. The fat droplets in the natural WG composite emulsion are relatively large, requiring more time to hydrolyze, which hinders BC release; the release rate of the WG composite emulsion was only 62.45%.

We collected the micellar phase and determined the bioavailability of BC in various emulsions. The bioavailability of BC in the HT-WG compound emulsion was 79.48%, which was significantly higher than that in the natural WG compound emulsion 66.32%. This indicates that heat treatment of natural WG can increase the bioavailability of its active ingredients (β-carotene). Heat treatment alters the conformation of natural WG molecules, prevents oil droplet aggregation in gastric juice, and enhances lipase access to the lipid droplet surface. Compound emulsions are digested in the small intestine, and appropriate encapsulation can delay BC release during in vitro digestion, thereby improving bioavailability and ensuring absorption. As demonstrated by the above experiments, heat-treated HT-WG is more suitable as an encapsulation material for embedding the active ingredient (β-carotene), maintaining its stability in digestive fluids (acidic environment), and effectively delaying the release of the active ingredient (β-carotene) during in vitro digestion.

Conclusion

We analyzed the solubility, hydrophobicity, structural characteristics, emulsion stability, and digestive properties of emulsions containing β-carotene, based on natural WG and heat-treated HT-WG. Differences in walnut glutelin structure and emulsion properties were induced by heat treatment (60°C-100°C). Heat treatment causes the natural WG structure to aggregate, resulting in higher solubility, larger particle size, and greater surface hydrophobicity. The emulsifying activity of natural WG was enhanced; its internal structure underwent partial unfolding and aggregation; the fluorescence peak shifted toward the red region, and its intensity increased; the number of α-helices in the secondary structure of WG decreased significantly ($P < 0.05$), the proportion of β-sheets increased, and the lost α-helices were almost entirely converted into disordered structures. When comparing emulsions formed before and

after heating under the same oil content conditions, the WG emulsion exhibited significant separation, whereas the HT-WG emulsion had relatively smaller droplet sizes. Because heating changed the WG structure, HT-WG showed superior emulsification stability compared with natural WG. Simulation of the gastrointestinal digestion process revealed that for the same processing method and equivalent oil content, the emulsion particle size increased as digestion progressed. However, the changes in the HT-WG were smaller than those in the WG. The HT-WG emulsion inhibited digestion, with the effect most pronounced at a relatively high temperature (90°C).

Declarations

Consent for publication

Not applicable.

Competing interests

The authors declare no competing interests.

Funding

This research was funded by Joint special project of Qujing Science and Technology Bureau and Qujing Normal University for science and technology innovation - Construction of walnut protein-based active emulsions and their application in condiments (Project No.: KJLH2024YB05). Basic Research Plan Project of Yunnan Provincial Department of Science and Technology (General Project) - Study on the Regulation of Emulsion Interfacial Rheology and Controlled Release Mechanism of Active Components by Walnut Glutelin-Polysaccharide Copolymer Complexes (Project No.: 202601AT070009). Doctoral research start-up funds, grant number 2107458995X745 and 2107458985X745”.

Author Contribution

CRediT: Jing Wang: Visualization, Formal analysis, Funding acquisition, Writing - review and editing, Supervision; Qian Sun: Conceptualization, Data curation, Investigation, Methodology, Resources, Software, Funding acquisition, Writing - original draft, Validation, Project administration.

Acknowledgement

This research was funded by Joint special project of Qujing Science and Technology Bureau and Qujing Normal University for science and technology innovation - Construction of walnut protein-based active emulsions and their application in condiments (Project No.: KJLH2024YB05). Basic Research Plan Project of Yunnan Provincial Department of Science and Technology (General Project) - Study on the

Regulation of Emulsion Interfacial Rheology and Controlled Release Mechanism of Active Components by Walnut Glutelin-Polysaccharide Copolymer Complexes (Project No.: 202601AT070009). Doctoral research start-up funds, grant number 2107458995X745 and 2107458985X745".

Data Availability

The data collected or analyzed during the study are all available in this published article. The datasets are available from the corresponding author on reasonable request.

Supplementary Information

The supplementary information of this study has been uploaded.

References

1. Huang, K., Zeng, S. M., Zhang, M., Liang, H. W., Zhang, Y., Li, S., Cao, H. W., Zhao, W. Q., & Guan, X. (2025). Comparative analysis of different drying methods in the production of solid oat milk beverages: Insights into physicochemical properties and quality attributes. *Journal of Cereal Science*, *123*, 104168. http://dor.org/10.1016/j.jcs.2025.104168
2. Prates, L. L., Lei, Y. G., Refat, B., Zhang, W. X., & Yu, P. Q. (2018). Effects of heat processing methods on protein subfractions and protein degradation kinetics in dairy cattle in relation to protein molecular structure of barley grain using advanced molecular spectroscopy. *Journal of Cereal Science*, *80*(5), 212–220. http://dor.org/10.1016/j.jcs.2018.01.008
3. Guo, C. F., Zhang, Z. N., Chen, J. J., Fu, H. F., Subbiah, J., Chen, W. X., & Wang, Y. Y. (2017). Effects of radio frequency heating treatment on structure changes of soy protein isolate for protein modification. *Food & Bioprocess Technology*, *10*(8), 1574–1583. http://dor.org/10.1007/s11947-017-1923-2
4. Mori, T., Nakamura, T., & Utsumi, S. (2010). Gelation mechanism of soybean 11S globulin: Formation of soluble aggregates as transient intermediates. *Journal of Food Science*, *47*(1), 26–30. http://dor.org/10.1111/j.1365-2621.1982.tb11019.x
5. Alizadeh-Pasdar, N., & Li-Chan, E. C. (2000). Comparison of protein surface hydrophobicity measured at various pH values using three different fluorescent probes. *Journal of Agricultural Food Chemistry*, *48*(2), 328–334. http://dor.org/10.1021/jf990393p
6. Murayama, K., & Tomida, M. (2004). Heat-induced secondary structure and conformation change of bovine serum albumin investigated by Fourier transform infrared spectroscopy. *Biochemistry*, *43*(36), 11526–11532. http://dor.org/10.1021/bi0489154
7. Zhang, M., Zhu, S., Li, Q., Xue, D. J., Jiang, S., Han, Y., & Li, C. B. (2023). Effect of thermal processing on the conformational and digestive properties of myosin. *Foods*, *12*(6), 1249. http://dor.org/10.3390/foods12061249

8. Peram, M. R., Loveday, S. M., Ye, A. Q., & Singh, H. (2013). In vitro gastric digestion of heat-induced aggregates of β-lactoglobulin. *Journal of Dairy Science*, *96*(1), 63–74. http://dor.org/10.3168/jds.2012-5896
9. Liu, W. J., Feng, Y. T., Delaplace, G., André, C., & Chen, X. D. (2022). Effect of calcium on the reversible and irreversible thermal denaturation pathway of β-lactoglobulin. *Food Hydrocolloids*, *133*, 107943. http://dor.org/10.1016/j.foodhyd.2022.107943
10. Deng, Y., Govers, C., Tomassen, M., Hettinga, K., & Wichers, H. J. (2020). Heat treatment of β-lactoglobulin affects its digestion and translocation in the upper digestive tract. *Food Chemistry*, *330*(15), 127184. http://dor.org/10.1016/j.foodchem.2020.127184
11. Tang, J. Y., Wichers, H. J., & Hettinga, K. A. (2022). Heat-induced unfolding facilitates plant protein digestibility during in vitro static infant digestion. *Food Chemistry*, *375*(1), 131878. http://dor.org/10.1016/j.foodchem.2021.131878
12. Lin, Y., Pangloli, P., Meng, X. J., & Dia, V. P. (2020). Effect of heating on the digestibility of isolated hempseed (*Cannabis sativa* L.) protein and bioactivity of its pepsin-pancreatin digests. *Food Chemistry*, *341*(1), 126198. http://dor.org/10.1016/j.foodchem.2020.126198
13. Sun, Q., Ma, Z. F., Zhang, H. X., Ma, S. J., & Kong, L. M. (2018). Structural characteristics and functional properties of walnut glutelin as hydrolyzed: Effect of enzymatic modification. *International Journal of Food Properties*, *22*(1), 265–279. http://dor.org/10.1080/10942912.2019.1579738
14. Sze-Tao, K. W. C., & Sathe, S. K. (2000). Walnuts (*Juglans Regia*L): Proximate composition, protein solubility, protein amino acid composition and protein in vitro digestibility. *Journal of the Science of Food & Agriculture*, 2000, 80(9), 1393–1401. http://dor.org/10.1002/1097-0010(200007)80:9%3C1393::aid-jsfa653%3E 3.0.co;2-f
15. Pearce, K. N., & Kinsella, J. E. (1978). Emulsifying properties of proteins: Evaluation of a turbidimetric technique. *Journal of Agricultural & Food Chemistry*, *26*(3), 716–723. http://dor.org/10.1021/jf60217a041
16. Zheng, Y. M., Li, Z. Y., Zhang, C., Zheng, B. D., & Tian, Y. T. (2020). Effects of microwave-vacuum pre-treatment with different power levels on the structural and emulsifying properties of lotus seed protein isolates. *Food Chemistry*, *311*(5), 125932. http://dor.org/10.1016/j.foodchem.2019.125932
17. Chen, W. J., Ma, X. B., Wang, W. J., Lv, R. L., Guo, M. M., Ding, T., Ye, X. Q., Miao, S., & Liu, D. H. (2019). Preparation of modified whey protein isolate with gum acacia by ultrasound maillard reaction. *Food Hydrocolloids*, *95*(10), 298–307. http://dor.org/10.1016/j.foodhyd.2018.10.030
18. Liang, H. N., & Tang, C. H. (2014). Pea protein exhibits a novel Pickering stabilization for oil-in-water emulsions at pH 3.0. *LWT - Food Science & Technology*, *58*(2), 463–469. http://dor.org/10.1016/j.lwt.2014.03.023
19. Li, Z. Q., Dai, L., Wang, D., & Gao, Y. X. (2018). Stabilization and rheology of concentrated emulsions using the natural emulsifiers quillaja saponins and rhamnolipids. *Journal of Agricultural & Food Chemistry*, *66*(15), 3922–3929. http://dor.org/10.1021/acs.jafc.7b05291

20. Moharana, A. K., Selvam, M. K. P., Jena, S. R., Chandra, P. K., Busija, D. W., Samanta, L., & Sikka, S. C. (2025). Comparative proteomics of seminal exosomes reveals size-exclusion chromatography outperforms ultracentrifugation. *Biomedicines*, *13*(10), 2459. http://dor.org/10.3390/biomedicines13102459
21. Lakemond, C. M., De Jonghh, H. H., Hessing, M., Gruppen, H., & Voragen, A. G. (2000). Heat denaturation of soy glycinin: influence of pH and ionic strength on molecular structure. *Journal of Agricultural & Food Chemistry*, *48*(6), 1991–1995. http://dor.org/10.1021/jf9908704
22. Tang, S., Li, J., Huang, G., & Yan, L. (2021). Predicting protein surface property with its surface hydrophobicity. *Protein & Peptide Letters*, *28*(8), 938–944. http://dor.org/10.2174/0929866528666210222160603
23. Wang, W. Q., Yuan, P. P., Zhou, J. Y., & Gu, Z. H. (2021). Effect of temperature and pH on the gelation, rheology, texture, and structural properties of whey protein and sugar gels based on Maillard reaction. *Journal of Food Science*, *86*(4), 1228–1242. http://dor.org/10.1111/1750-3841.15659
24. Liu, F., & Tang, C. H. (2014). Emulsifying properties of soy protein nanoparticles: Influence of the protein concentration and/or emulsification process. *Journal of Agricultural & Food Chemistry*, *62*(12), 2644–2654. http://dor.org/10.1021/jf405348k
25. Wang, J. M., Xia, N., Yang, X. Q., Yin, S. W., Qi, J. R., He, X. T., Yuan, D. B., & Wang, L. J. (2012). Adsorption and dilatational rheology of heat-treated soy protein at the oil-water interface: Relationship to structural properties. *Journal of Agricultural & Food Chemistry*, *60*(12), 3302–3310. http://dor.org/10.1021/jf205128v
26. Nyemb, K., Guérin-Dubiard, C., Dupont, D., Jardin, J., Rutherfurd, S. M., & Nau, F. (2014). The extent of ovalbumin in vitro digestion and the nature of generated peptides are modulated by the morphology of protein aggregates. *Food Chemistry*, *157*, 429–438. http://dor.org/10.1016/j.foodchem.2014.02.048
27. Verma, K., Semwal, A., Soni, P., & Bhatia, R. (2021). Perspectives of infrared spectroscopy in quantitative estimation of proteins. *Current Analytical Chemistry*, *17*(5), 689–707. http://dor.org/10.2174/1573411016999200917113433
28. Zhao, M. M., Wu, X. J., Li, F., Li, H. L., & Wu, W. (2023). Effect of rice bran rancidity on the structural characteristics and rheological properties of rice bran protein fibril aggregates. *Food Hydrocolloids*, *144*, 108959. http://dor.org/10.1016/j.foodhyd.2023.108959
29. Ren, S., Rodriguez-Saona, L., & Giusti, M. M. (2022). Analyzing the interaction between anthocyanins and native or heat-treated whey proteins using infrared spectroscopy. *Molecules*, *27*(5), 1538–1545. http://dor.org/10.3390/molecules27051538
30. Guilmineau, F., & Kulozik, U. (2006). Impact of a thermal treatment on the emulsifying properties of egg yolk. Part 1: Effect of the heating time. *Food Hydrocolloids*, *20*, 1105–1113. http://dor.org/10.1016/j.foodhyd.2005.12.005
31. Guilmineau, F., & Kulozik, U. (2006). Impact of a thermal treatment on the emulsifying properties of egg yolk. Part 2: Effect of the environmental conditions. *Food Hydrocolloids*, *20*, 1114–1123.

http://dor.org/10.1016/j.foodhyd.2005.12.006

32. Gantumur, M. A., Sukhbaatar, N., Shi, R. J., Hu, J. L., Bilawal, A., Qayum, A., Tian, B., Jiang, Z. M., & Hou, J. C. (2023). Structural, functional, and physicochemical characterization of fermented whey protein concentrates recovered from various fermented-distilled whey. *Food Hydrocolloids*, *135*(2), 108130. http://dor.org/10.1016/j.foodhyd.2022.108130
33. Keerati-u-rai, M., & Corredig, M. (2009). Heat-induced changes in oil-in-water emulsions stabilized by soy protein isolate. *Food Hydrocolloids*, *23*, 2141–2148. http://dor.org/10.1016/j.foodhyd.2009.05.010
34. Xie, H. J., Xiang, C. Y., Li, Y., Wang, L. H., Zhang, Y. T., Song, Z. J., Ma, X. J., Lu, X. Y., Lei, Q. F., & Fang, W. J. (2019). Fabrication of ovalbumin/κ-carrageenan complex nanoparticles as a novel carrier for curcumin delivery. *Food Hydrocolloids*, *89*(4), 111–121. http://dor.org/10.1016/j.foodhyd.2018.10.027
35. Zou, L. Q., Zheng, B. J., Zhang, R. J., Zhang, Z. P., Liu, W., Liu, C. M., Xiao, H., & Mcclements, D. J. (2016). Enhancing the bioaccessibility of hydrophobic bioactive agents using mixed colloidal dispersions: curcumin-loaded zein nanoparticles plus digestible lipid nanoparticles. *Food Research International*, *81*(4), 74–82. http://dor.org/10.1016/j.foodres.2015.12.035
36. Li, Y., & McClements, D. J. (2010). New mathematical model for interpreting pH-stat digestion profiles: impact of lipid droplet characteristics on in vitro digestibility. *Journal of Agricultural & Food Chemistry*, *58*(13), 8085–8092. http://dor.org/10.1021/jf101325m
37. Singh, H., & Ye, A. Q. (2013). Structural and biochemical factors affecting the digestion of protein-stabilized emulsions. *Current Opinion in Colloid & Interface Science*, *18*(4), 360–370. http://dor.org/10.1016/j.cocis.2013.04.006
38. Guo, Q., Su, J. Q., Shu, X., Yuan, F., Mao, L. K., Liu, J. F., & Gao, Y. X. (2020). Production and characterization of pea protein isolate-pectin complexes for delivery of curcumin: effect of esterified degree of pectin. *Food Hydrocolloids*, *105*, 105777. http://dor.org/10.1016/j.foodhyd.2020.105777

Figures

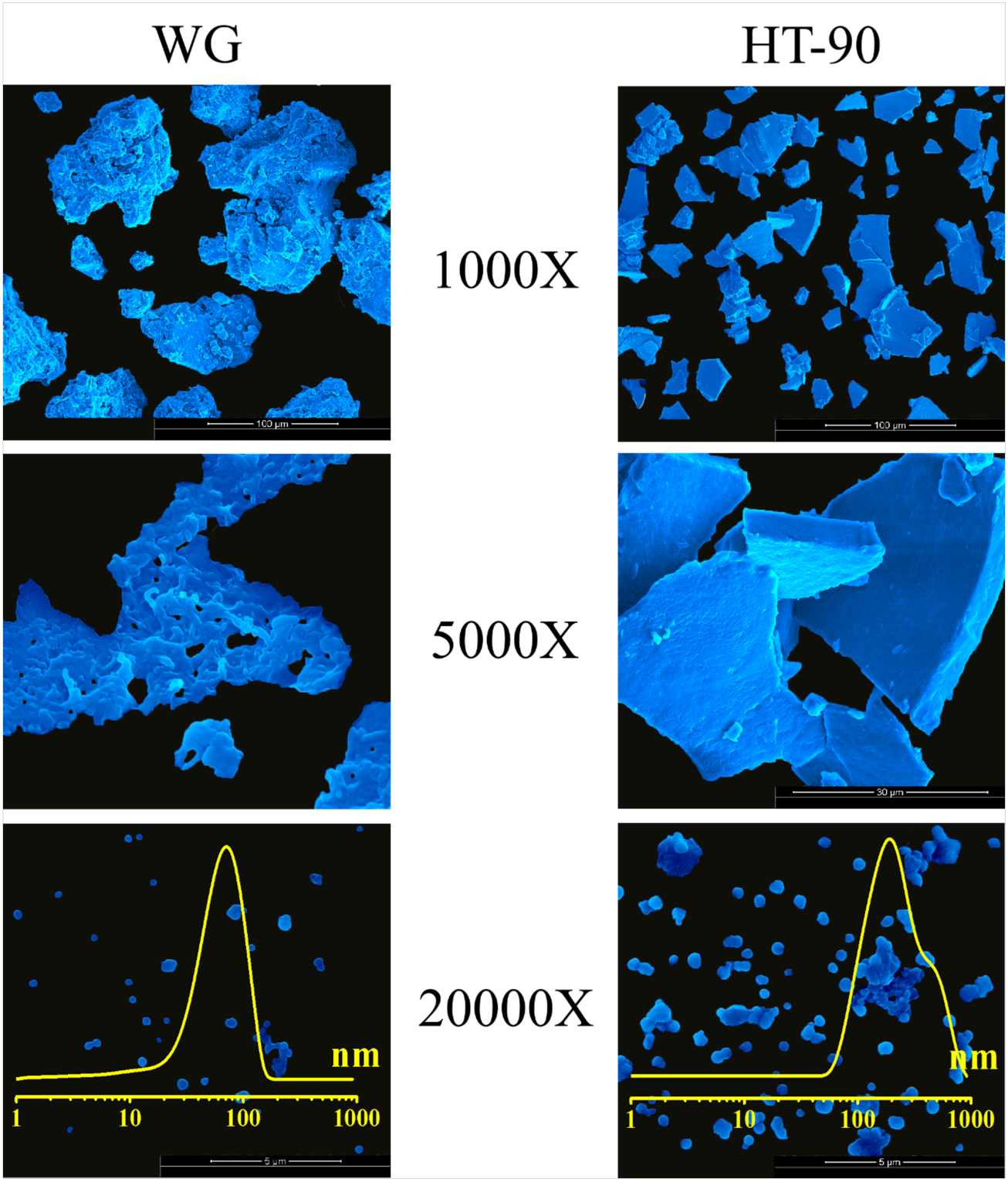


Figure 1

Effect of heat treatment on the particle size distribution of WG. WG is walnut glutelin; HT-90 is heat-treated walnut glutelin (90°C, 30 min).

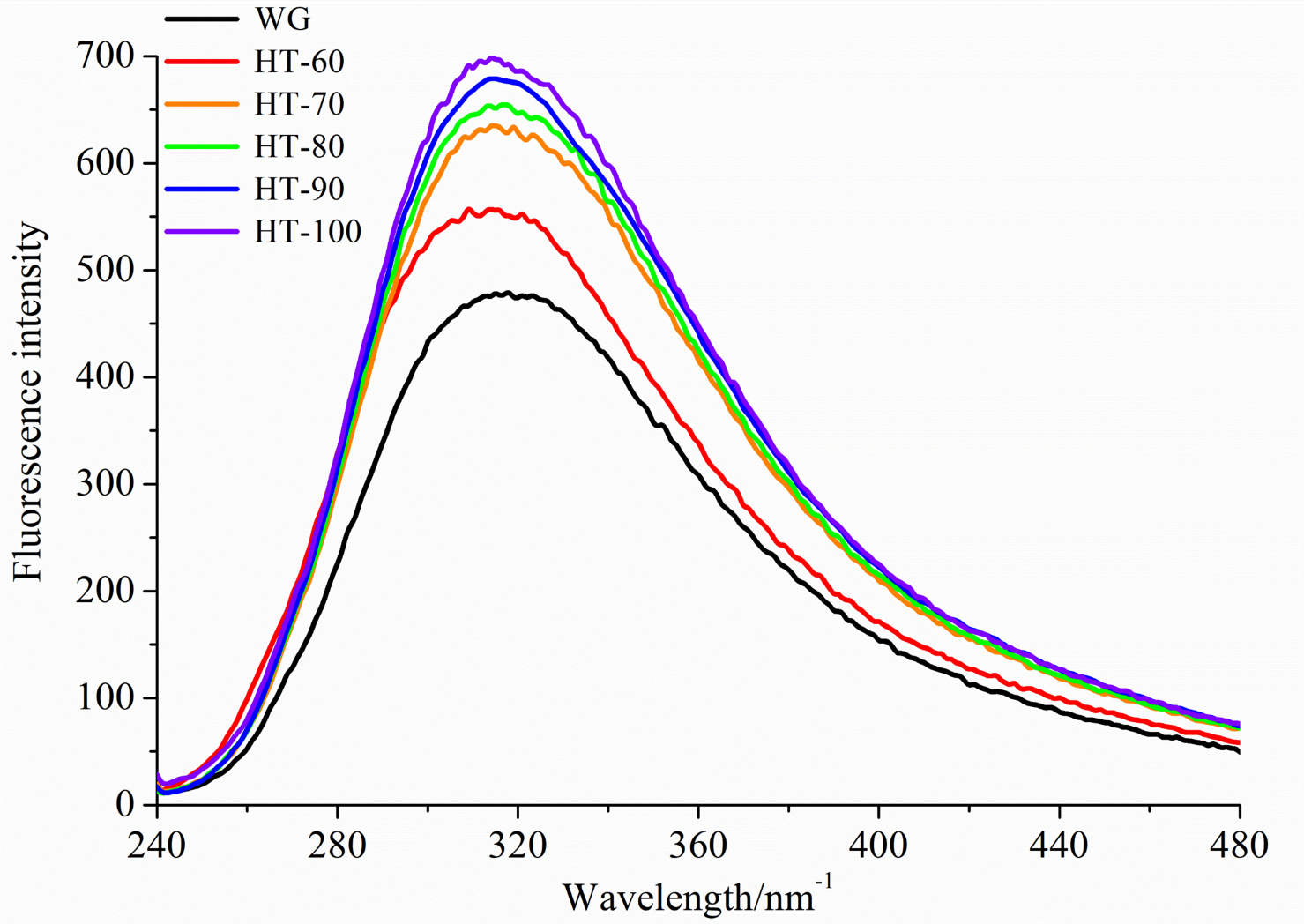


Figure 2

Fluorescence spectroscopy Analysis. WG is walnut glutelin; black, red, orange, green, blue, and purple represent WG, HT-60, 70, 80, 90, and 100°C, respectively, for 30 min.

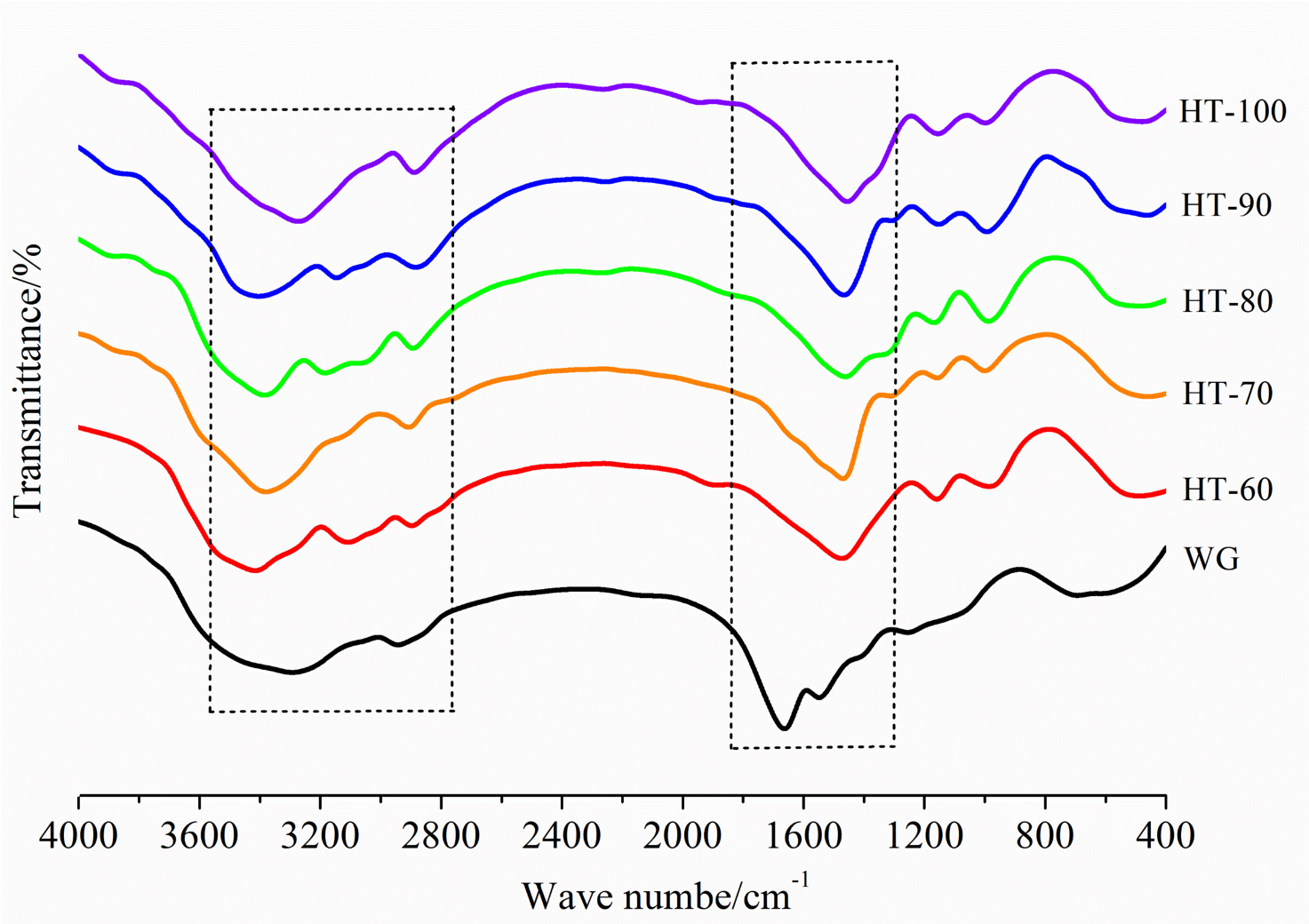


Figure 3

Infrared spectroscopy analysis. WG is walnut glutelin; black, red, orange, green, blue, and purple represent WG, HT-60, 70, 80, 90, and 100°C, respectively, for 30 min.

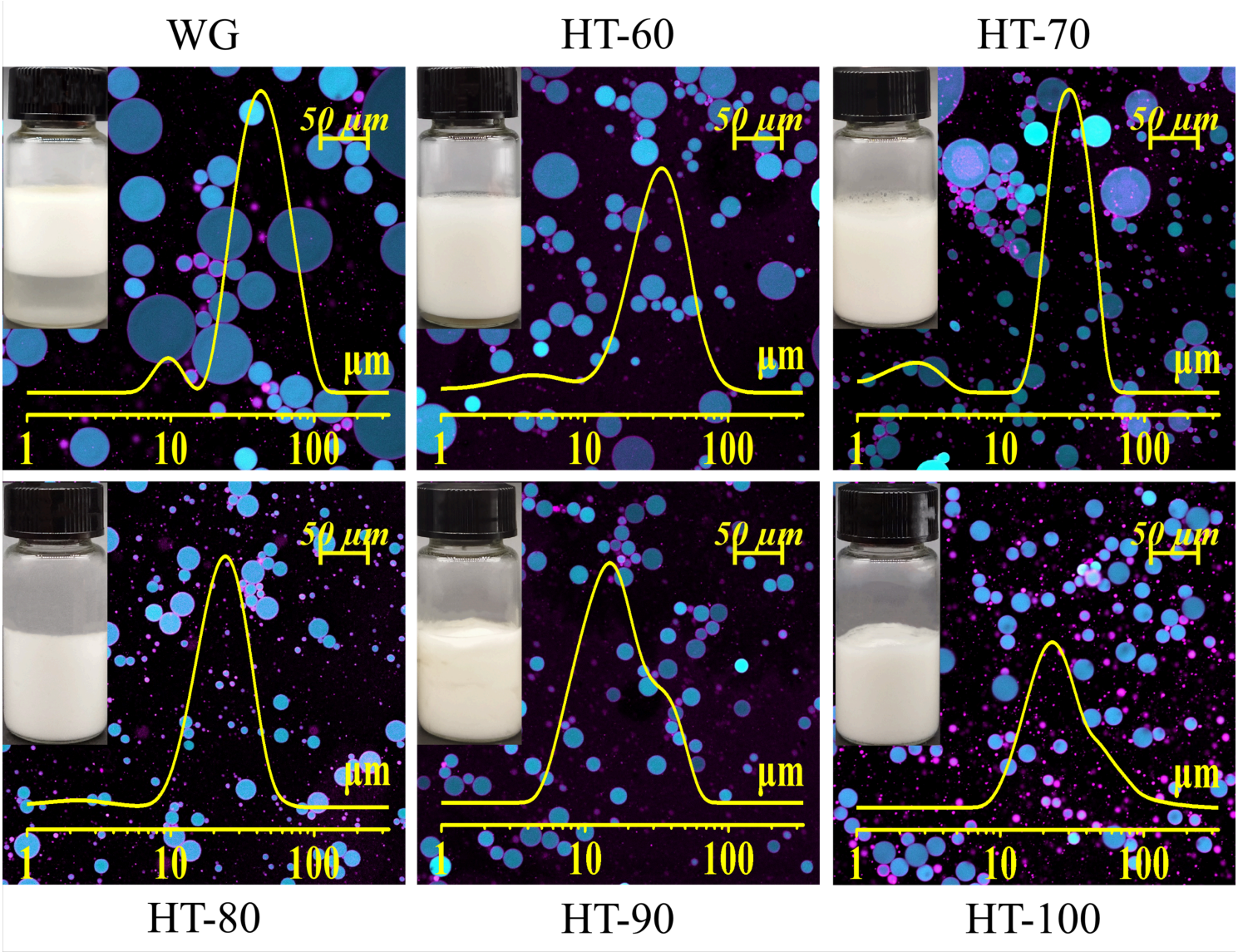


Figure 4

Direct photographs of WG emulsion (stored at 25°C for 24 h), particle size distribution, and microstructure (20 X). Protein particle signal was set to pink (488 nm), and the oil-phase droplets are visualized in blue (leaning toward blue-green, 633 nm). WG is walnut glutelin; c = 1.0%; ϕ = 20. Heat treatment: 60, 70, 80, 90, 100°C for 30 min.

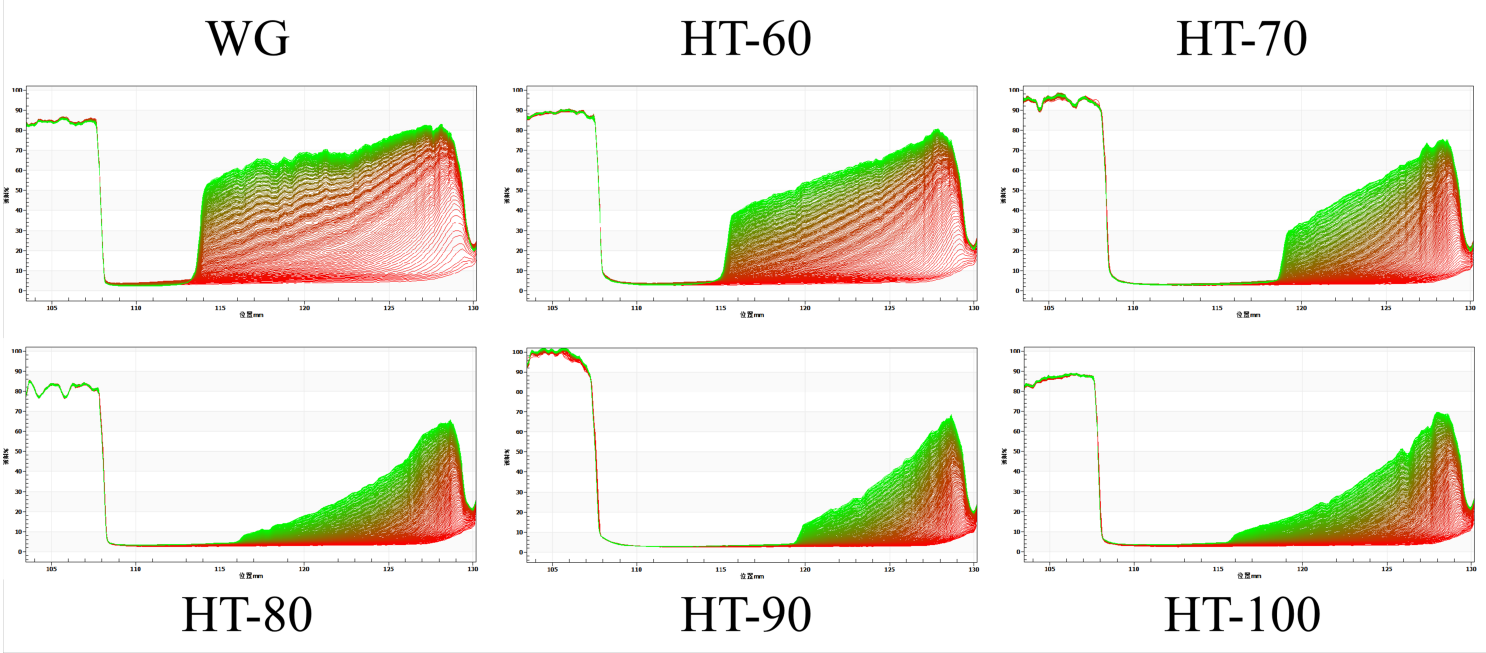


Figure 5

Emulsion stability analysis. WG is walnut glutelin; c = 1.0%; ϕ = 20. Heat treatment: 60, 70, 80, 90, 100°C for 30 min.

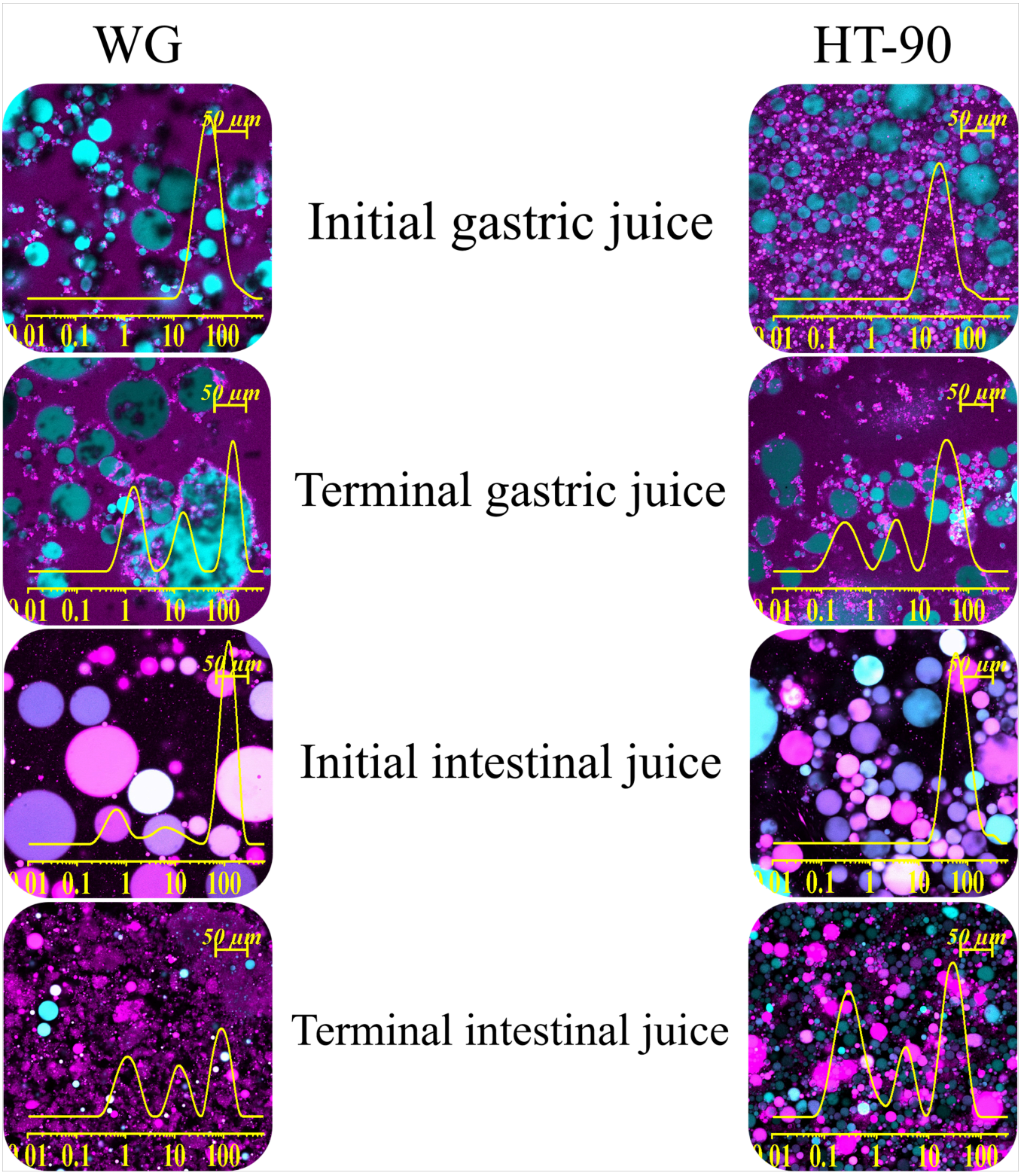


Figure 6

Microscopic diagram of WG composite emulsion digestion (20 X). WG is walnut glutelin; HT-90 is heat-treated walnut glutelin (90°C, 30 min); c = 1.0%; ϕ = 20.

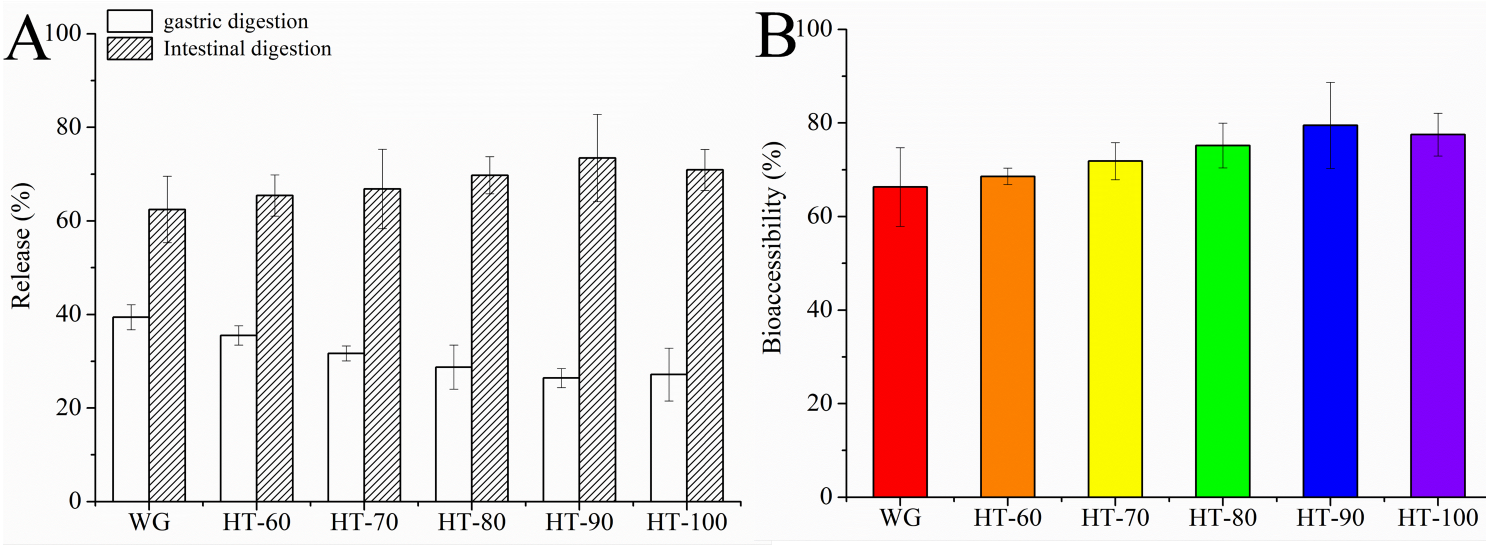


Figure 7

In vitro release and bioavailability of WG composite emulsion. WG stands for walnut glutelin; c = 1.0%; ϕ = 20. Heat treatment: 60, 70, 80, 90, 100°C for 30 min.